Christian Koerner, Max L. Tietze, Torben Menke, and Karl Leo*

MOLECULAR DOPING FOR ORGANIC ELECTRONIC DEVICES: DOPING CONCEPT AND INFLUENCE OF TRAP LEVELS

ABSTRACT

We review recent progress in the understanding of molecular doping of organic semiconductors. A statistical description of the doping process using an acceptor level E_A and additionally considering charge carrier trap states allows to quantitatively model Fermi level shifts observed in photoelectron spectroscopy. A trap filling, saturation, and reserve regime is observed: A steep rise of the Fermi level for doping concentrations above the trap concentration as well as low doping efficiencies at high doping concentrations can be well explained by the model. Doping can also be characterized using Seebeck measurements, giving qualitatively similar results for different combinations of matrix and dopant molecules. In combination with conductivity measurements, the transport energy is exemplarily determined for n-doped C_{60} at 210meV below the center of the LUMO density of states. Finally, the importance of trap level characterization for device modeling and material purity analysis is emphasized.

A INTRODUCTION

Organic electronics is an emerging technology that has attracted great interest in the last decades. The primary goal is not to replace existing technologies, but to create a new form of electronics which cannot be realized by standard inorganic semiconductor technologies. Important factors are the feasibility of, e.g., flexible devices, broad tunability of material properties, the possibility of low-temperature roll-to-roll processing, and the low weight of final products. The range of applications starts with organic light emitting diodes (OLED), which are already established on the display market, moving on to organic solar cells (OSC) and organic transistors (OFET), currently entering the market. The basis of all those technologies are π-conjugated organic molecular or polymeric materials exhibiting semiconducting properties. In contrast to inorganic semiconductors, their transport properties are fundamentally different, particu-

larly, charge carrier mobilities are orders of magnitude lower than in inorganic crystalline solids. The reasons are the weak intermolecular coupling due to van-der-Waals forces, a strong charge localization due to reduced screening of the charge, a broad density of states (DOS) due to the disordered nature of thin films, and further (shallow or deep) trap states due to impurities or strong morphological disorder. Additionally, the intrinsic charge carrier concentration is rather low due to the large band gap. Unwanted impurities create trap states of comparable density, such that the overall conductivity is low.

To drive high currents through OFETs or OLEDs or efficiently extract charge carriers in OSCs, doping was introduced equivalent to inorganic semiconductors.[1, 2, 3] The resulting increase in conductivity is due to an increased free charge carrier concentration and often also a higher mobility, leading to less transport losses and an Ohmic behavior at device contacts[4]. Doping was also used to realize organic tunnel diodes for a precise tuning of the breakdown voltage[5, 6] as well as for defining the threshold voltage in organic inversion and depletion transistors[7]. Recently, doping was used for in-depth investigations of the trap distributions by controlled trap filling such that trapped charges can respond to an electrical signal.[8, 9]

Despite the success of this concept in the last years, the doping process itself is still not fully understood. Previous works have suggested different physical mechanisms to explain, e.g., the usually observed rather low doping efficiencies.[10, 11, 12] However, as we discuss below, in many cases the concepts from inorganic semiconductors can reasonably describe the experimental observations.

Technically, the challenge remains to find suitable dopants with either deep energy levels for p-doping, or high levels for n-doping. Especially the latter leads to instability of most n-dopants against oxidation, such that synthesis and handling of those compounds must be performed under exclusion of any atmospheric contact. Therefore, new material concepts were developed in order to find air stable dopant compounds that develop their doping capability just upon processing, like molecular dimers that dissociate upon thermal evaporation.[13, 14, 15, 16]

In this paper, we review the common understanding of the doping mechanism in organic small molecule semiconductors. In particular, we summarize our recent experimental progress and advances in the description of the doping process and the

Dr, Christian Koerner
Dr. Max Tietze
Dr. Torben Menke
Prof. Dr. Karl Leo
Institut für Angewandte Photophysik
Technische Universität Dresden, Dresden, Germany
* corresponding author: leo@iapp.de

doping efficiencies. Furthermore, we will highlight the importance of trap states for the doping process, how those trap states can be analyzed, and how doping can contribute to their quantitative characterization. For more in-depth information about molecular doping and its history, we refer to previous works.[2, 12, 17, 18, 19, 20]
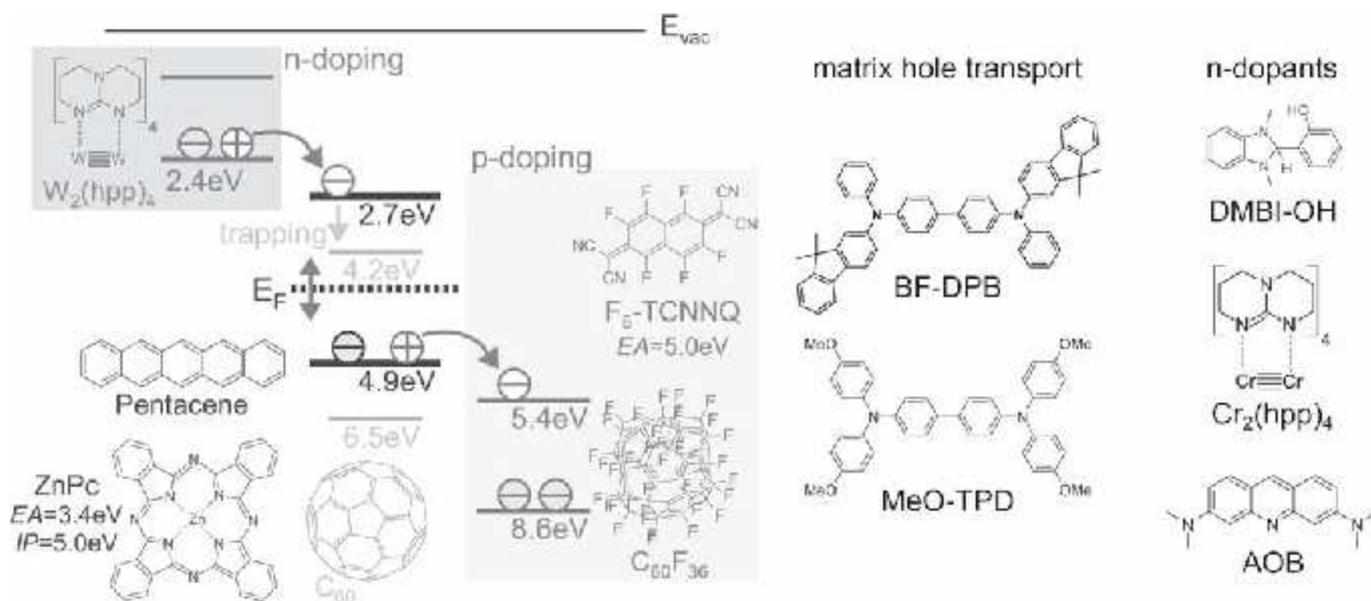
B DOPING IN ORGANIC SEMICONDUCTORS

In organic semiconductors, doping is achieved by mixing dopant molecules into a matrix by coevaporation or spin coating. In the simplest picture, doping can be predicted from the energy levels of matrix and dopant, which is sketched in Figure 1. For n-doping, the HOMO of the dopant must be higher than the LUMO of the matrix. Similarly, for p-doping the LUMO of the dopant must be lower than the HOMO of the matrix. However, there are more factors influencing the doping efficiency, like the intermolecular coupling constants for the charge transfer between matrix and dopant, the efficiency of charge separation of the bound electron-hole pair after charge transfer, i.e., the permittivity of the matrix[10], morphology changes in the matrix upon introducing dopants[21], or the doping concentration itself[10].

Typical matrix and dopant materials for p- and n-doping are shown in Figure 1. Particularly interesting are ambipolar matrix materials that can be both p- and n-type doped to realize homojunctions like for inorganic semiconductors.[22, 23] Here, the challenge is to find suitable dopants, because then the p-dopant must be very low in energy, whereas the n-dopant must be very high in energy.

The charge generation process upon doping is still not fully understood. Early measurements with infrared spectroscopy methods indicated that the charge transfer between dopant and matrix can be close to 100% efficient. However, this only leads to a charge-transfer state, where electron and hole are still Coulomb-bound. The final doping efficiency, i.e., the ratio between free charge carrier density and introduced dopant density, is only in the order of a few percent.[2, 24, 10] Different models were supposed to describe these low efficiencies, e.g., hybridization of matrix and dopant[11], a high Coulombic binding between electron and hole due to inefficient screening following the charge transfer[10], dopant aggregation[25], or a shift of the dopant energy levels upon ionization[26].

Doping can be validated by various measures. Most important for the application in electronic devices are two aspects: First, the increase of the conductivity by several orders of magnitude, reducing the Ohmic resistance of bulk layers, and second, thin space charge layers, allowing efficient Ohmic contacts by tunneling. Typical conductivities are in the range of 10^{-6}-10^{-3} S/cm for p-doped films[24, 27, 28] and 10^{-4}-10 S/cm for n-doped films[14, 29, 30, 13, 31]. The higher numbers for n-doped films are mainly due to the use of high-mobility matrix materials like fullerenes, compared to rather amorphous hole transport materials. However, similarly high conductivities of 10^{-1} S/cm were reported for p-pentacene.[21] For most thin-film devices, conductivities in the order of 10^{-5} S/cm are sufficient to ensure low series resistances. However, the ultra-high conductivity in C_{60} films even allows the use as transparent alternative electrodes, at least for small areas.[32] Besides conductivity measurements, the shift of the Fermi level versus the LUMO level for n-doping or versus the HOMO level for p-doping can be measured by ultra-violet photoelectron spectroscopy (UPS). Thermovoltage (Seebeck) measurements reveal the Seebeck energy, which is the energy difference between the Fermi energy and the average transport level. The sign furthermore identifies p- or n-type transport (i.e., doping). Finally, the actual charge transfer between matrix and dopant is visualized by IR spectroscopy due to the shift of vibrational energies upon charging[33, 2], electron spin resonance, ^{19}F-NMR, or Raman spectroscopy.[34]
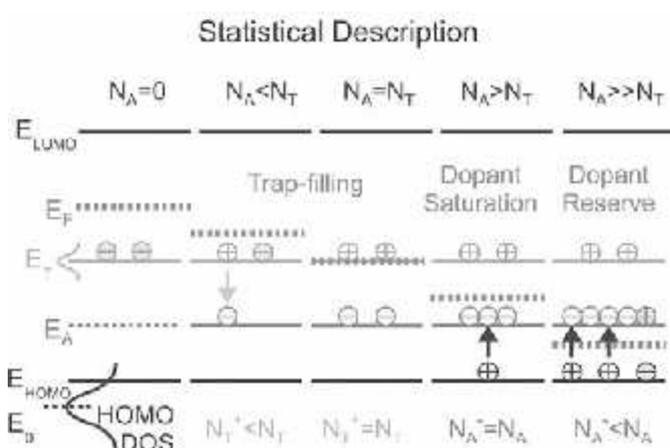

Figure 1: Sketch of the doping process in organic semiconductors. For n-doping, the HOMO level of the dopant must be higher than the LUMO level of the matrix for efficient charge transfer. Similarly, for p-doping the LUMO of the dopant must be lower than the HOMO of the matrix to allow electron transfer to the dopant, leaving a hole in the matrix. Typical matrix materials and dopants are shown as well. Reprinted with permission from Advanced Functional Materials, 25, 2701, 2015. Copyright 2015, John Wiley & Sons, Inc.

C A STATISTICAL DESCRIPTION OF THE DOPING PROCESS

In previous experiments, it was shown that upon doping the Fermi level shifts towards the respective transport level (HOMO for p-doping), but saturates at several hundred meV above the actual HOMO energy (Fermi level pinning).[24] This energetic distance does not depend on the dopant, but on the matrix molecule. It was concluded that pinning of the Fermi level is due to an extended tailing of the density of states into the gap of the semiconductor. However, a detailed description of these states was not given.

Recently, Tietze et al. used a statistical approach in analogy to classical semiconductor physics to describe both the Fermi level pinning as well as the strong increase of the Fermi level shift at low doping concentrations.[10] For the description in the case of p-doping, the authors introduced intragap hole trap states at an energy E_T and an acceptor level for the p-dopants E_A (see the sketch in Figure 2 for the p-doping case and the correspondingly measured Fermi level shift respectively change of the hole injection barrier with increasing doping concentration in Figure 3a). At low doping concentrations, where the dopant density is smaller than the trap density, the Fermi level shifts from its intrinsic position towards the trap level where it is pinned: The holes introduced by the p-dopants only fill up the trap states (trap filling, trap limitation). At $N_A=N_T$, the Fermi level aligns with the trap level. A further increase of the doping concentration leads to a rapid shift of the Fermi level towards the transport level (dopant saturation). At very high doping concentration, the doping efficiency strongly decreases leading to a saturation of the Fermi level (dopant reserve).

Using semiconductor statistics and assuming a Gaussian distribution of trap states allows a quantitative description of the measurement by varying the trap depth E_T, the trap density N_T, the width of the trap state distribution σ_T, and the acceptor level E_A: changing E_T controls the Fermi level at low doping concentrations, whereas E_A sets the Fermi level at high concentrations. N_T defines the doping concentration, where the strong Fermi level shift is observed, and σ_T determines the slope of the Fermi level shift at lower doping concentrations. The optimal fit parameters for the example of p-doped MeO-TPD are given in the caption to Figure 3. However, the turnover from the steep rise to the saturation of the Fermi level is still not well modeled. Therefore, Tietze et al. extended the HOMO states by exponential tail states reaching into the gap of the matrix. The characteristic parameters of this distribution were determined from measuring the UPS emission signal with high precision in the gap (see Figure 3d).

Finally, calculated doping efficiencies are compared to experimentally determined values (see Figure 3b). The doping efficiency is defined as the ratio between the hole density and
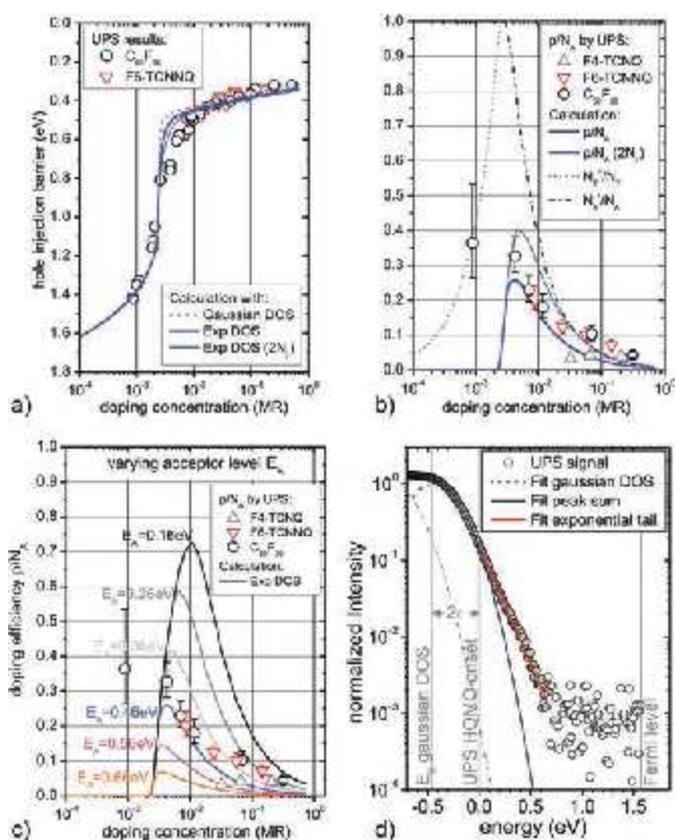
Figure 3: UPS measurements on MeO-TPD p-doped with F_6-TCNNQ or $C_{60}F_{36}$. The doping concentration is given here as molar ratio (MR) between dopant and matrix molecules. a) The hole injection barrier decreases with increasing doping concentration, which is equivalent to a shift of the Fermi level towards the HOMO of MeO-TPD. The solid line is obtained using E_A = 0.46 eV, E_T = 1.35 eV, N_T = $3.5 \cdot 10^{18}$ cm^{-3}, and σ_T = 0.15 eV. The parameters for the additional exponential tail states (blue lines) are determined from d). b) Calculation of trap occupation N_T^+/N_T, dopant activation N_A^-/N_A, and doping efficiency p/N_A in dependence of the doping concentration. The experimental values are taken from UPS measurements. c) Calculation of the doping efficiency for different acceptor levels E_A, which changes the maximum value, but not the decrease towards high doping concentration. d) Sensitive UPS measurement in the gap of the semiconductor. The emission signal from the HOMO does not follow a pure Gaussian distribution, but is extended by an exponential tail. The fit parameters E_β = -0.09 eV, β = 0.139 eV, N_β = $1.07 \cdot 10^{20}$ cm^{-3} are used in a). Reprinted with permission from Tietze et al., Physical Review B, 86, 035320, 2012. Copyright 2012 by the American Physical Society.

Figure 2: Sketch of the Fermi level shift with increasing doping concentration for the case of p-doping. Here, E_{LUMO} and E_{HOMO} correspond to the energies of the matrix. E_T and E_A are extracted from the statistical analysis and do not directly correspond to molecular energy levels of matrix or dopant. At low doping concentrations, the introduced dopants fill the trap states at energy E_T. The Fermi level shifts towards the trap level until $N_A=N_T$. The doping efficiency is close to zero as only traps are filled instead of the creation of free charge carriers. For $N_A>N_T$, the Fermi level rapidly moves towards the HOMO level. At high dopant density, i.e., when the Fermi level crosses the statistical acceptor level E_A of the dopants, Fermi-Dirac statistics demands the deoccupation of the dopants, leading to a reduced doping efficiency. Reprinted with permission from Advanced Functional Materials, 25, 2701, 2015. Copyright 2015, John Wiley & Sons, Inc.

the introduced dopant density as p/N_A. At low concentrations, the doping efficiency is zero because of the trap limitation. The maximum doping efficiencies obtained are in the range of 30%, which is defined by the determined acceptor level[§]. In principle, higher efficiencies could be reached for lower acceptor levels E_A closer to the HOMO center [8, 35], which is shown in Figure 3c, corresponding to the case of shallow impurities in single-crystal silicon[36]. However, irrespective of E_A, the doping efficiency strongly decreases at high doping concentrations, which is an intrinsic property of the statistics of the system. As soon as the Fermi level crosses the acceptor level, the occupation probability of E_A (for electrons) decreases, leading to a slower increase of the hole density in the HOMO of the matrix and, therefore, a reduced doping efficiency at high doping concentrations.

The authors also give a microscopic interpretation for this statistical description. The energy of the acceptor level is related to the energy needed for dissociating the charge pair at a dopant-matrix couple following the initial charge transfer, where the latter is usually assumed to be close to 100% efficient. The probability of generating a free charge carrier is, therefore, defined by E_A, i.e., independent of the doping concentration. In contrast, the capture probability of a free hole at an ionized dopant increases with the amount of ionized dopants, reducing the average density of free holes. The interplay between capture and release limits the doping efficiency and leads to the Fermi level saturation at high doping concentrations.
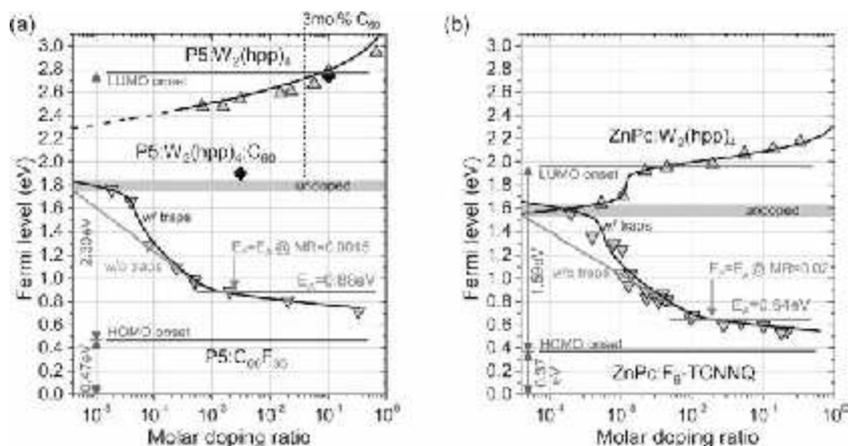
According to the above explanations, the Fermi level shift with varying doping concentration can be divided into three distinct regions (see Figure 2): trap limitation at low concentrations, dopant saturation for $E_F < E_T$ ($N_A > N_T$, indicated by the strong Fermi level shift), and the dopant reserve for $E_F < E_A$. The first regime is particularly difficult to resolve due to the low doping concentrations needed. By introducing a rotating shutter with a transmission of 5% in the evaporation system, it was possible to further reduce the molar doping ratio by one order of magnitude down

to 10^{-5} and clearly resolve this regime.[35] Both of the systems investigated, i.e., pentacene(P5):$C_{60}F_{36}$ and ZnPc:F_6-TCNNQ, show the three characteristic regimes, but differ in the statistical parameters obtained (see Figure 4). In contrast to p-doping, n-doping of the same matrix materials shows only dopant saturation (and trap filling), indicating high doping efficiencies even at high doping concentrations. The Fermi level even crosses the LUMO onset at high doping concentration, because it does not seem to be pinned by a donor level E_D. The trap limitation is as well observed for n-ZnPc, whereas it is not visible for n-P5 in the investigated range of doping concentrations.

D CONDUCTIVITY AND SEEBECK MEASUREMENTS TO STUDY CHARGE CARRIER MOBILITY, CHARGE CARRIER DENSITY, AND TRANSPORT ENERGY

The conductivity σ depends on the charge carrier density n and the mobility μ: $\sigma = en\mu$. Upon doping, the conductivity is increased due to the increase of n. A constant doping efficiency would give a linear increase of the conductivity. However, doping also increases μ due to trap filling or a positive dependence of $\mu(n)$. In combination, those effects should lead to a superlinear increase of the conductivity at low doping concentrations. Additionally, the morphology of the matrix can significantly be influenced at high doping concentrations, reducing the charge carrier mobility and, therefore, also the conductivity.[21] Finally, as explained above the doping efficiency is not constant, but decreases at high concentrations.

Menke et al. investigated different combinations of matrix materials and dopants for both n- and p-doping. [27, 30, 13] The obtained dependencies of the conductivity on the doping concentration are shown in Figure 5. In n-doped C_{60}, the slope of the conductivity increase is close to unity for most dopants except for DMBI-POH. As the matrix material is identical, the different behavior is attributed to a different dependence of the doping efficiency on the doping concentration as compared to the other dopants. Particularly noticeable is the decrease of the conductivity at high doping concentrations for the bulky dopants $W_2(hpp_4)$ and $Cr_2(hpp)_4$. This decrease is attributed to morphology changes in the matrix, which is more prominent for the larger and heavier dopants because they take a much higher volume fraction at the same molar doping ratio compared to the smaller dopants AOB and DMBI-POH. This effect is similarly visible in Figure 5b when comparing the two p-dopants F_6-TCNNQ and $C_{60}F_{36}$. For the smaller and lighter dopant, the conductivity increases even at high concentrations, whereas a decrease is observed for $C_{60}F_{36}$ independent of the matrix material used. A decrease in the conductivity could furthermore be reasoned by clustering of dopants, reducing the effective doping concentration at values approaching unity.

Figure 4: UPS measurements of the Fermi level in dependence of the doping ratio for two matrix materials that are both p- or n-doped: pentacene (P5) (a) and ZnPc (b). The solid lines are fits according to the model used by Tietze et al. [10, 35] The Fermi level is given with respect to the peak positions of the HOMOs and LUMOs, respectively. In (a), black points indicate triple evaporation of C_{60} as electron traps into P5:$W_2(hpp)_4$, showing that the Fermi level is pinned to the intrinsic case if the C_{60} trap concentration is higher than the concentration of the $W_2(hpp)_4$ dopant. Reprinted with permission from Advanced Functional Materials, 25, 2701, 2015. Copyright 2015, John Wiley & Sons, Inc.

[§] Note that without taking exponential tail states into account, the experimental values cannot be reproduced and the maximum doping efficiency is only 0.5%.
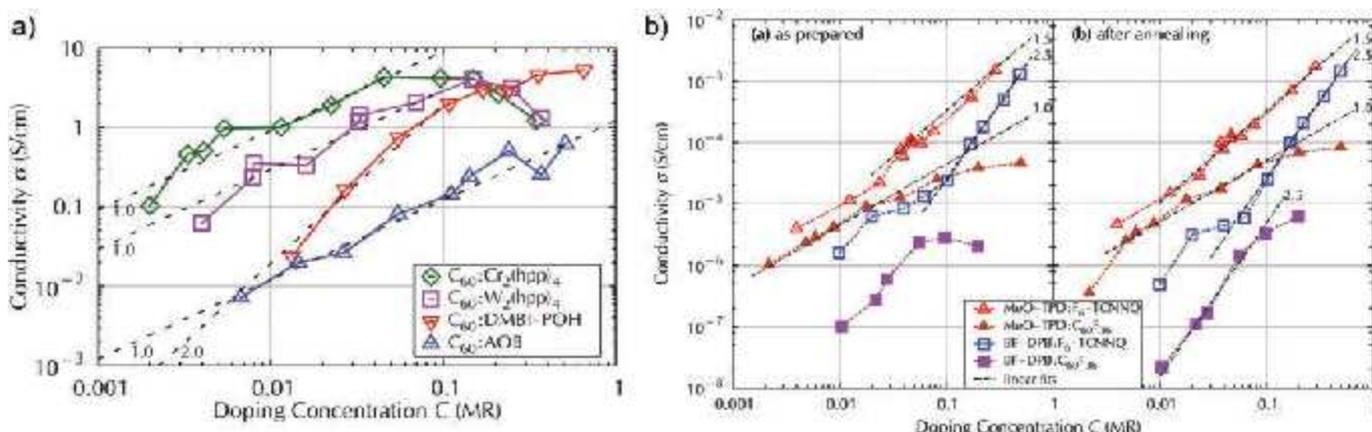
Figure 5: a) Conductivity of C_{60} n-doped using different dopant molecules at varying doping concentration. b) Conductivity of two different p-dopants in two different matrix materials at varying doping concentration as prepared and after an annealing step (for details, please refer to the original publication). Graph a) is reprinted from [44] with permission from the author. The data was further published in [37]. Graph b) is reprinted from Organic Electronics, 15, 365, 2014, Copyright 2014, with permission from Elsevier.

Doping can further be validated by Seebeck measurements. A spatial temperature gradient over a semiconductor sample induces a voltage difference that is proportional to the difference between the Fermi energy and the transport energy in the sample, which is called Seebeck energy E_S. Therefore, repeating this measurement for different doping concentrations serves as a complementary method to UPS to show the Fermi level shift upon doping. Figure 6 and 7 show determined Seebeck energies for p-doped and n-doped samples, respectively. The reduction of the Seebeck energy indicates the shift of the Fermi level towards the transport level. In most cases, n-doping gives smaller Seebeck energies than p-doped samples, indicating a higher doping efficiency as already concluded from UPS measurements where the Fermi level comes much closer to the transport level for n-doping compared to p-doping (cp. Figure 4).

The combination of Seebeck and temperature dependent conductivity measurements can be used to derive conclusions about changes in the transport properties upon doping. Temperature dependent conductivity measurements reveal

an activated transport that follows an Arrhenius behavior. The activation energies E_{act} contain both the activation of the charge carrier density (dopant activation) as well as a thermal activation of the mobility (increased charge carrier density and the thermal activation of hopping transport). The determined activation energies are compared to the Seebeck energies for n-doped C_{60} films in Figure 7. For low doping concentrations, both values are in good agreement, indicating that the dopant activation is the limiting factor. For higher concentrations, the introduction of the dopants leads to a disruption of the C_{60} matrix. The effect for charge transport is a reduction of the mobility and an increase in E_{act}.

In contrast to n-doped C_{60}, where typical activation energies between 40 and 250meV are found[30, 13], p-doped samples show much higher values in the range of 200-400meV[27], indicating both lower doping efficiencies (deeper dopant levels E_A) as well as lower charge carrier mobilities, especially for the typically more amorphous hole transport materials like MeO-TPD and BF-DPB.

In principle, the conductivity values can be used to derive either n or μ, if one of the two parameters is known. As the exact doping efficiencies are mostly unknown, a lower limit (LL) for the mobility can be obtained by assuming a maximum dop-
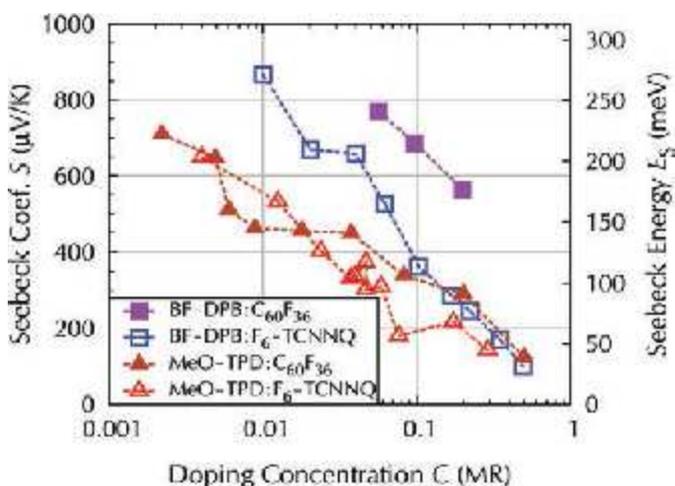

Figure 6: Seebeck coefficients S and derived Seebeck energies E_S from Seebeck measurements for different doping concentrations (given as molar ratio) on different p-doped systems (BF-DPB or MeO-TPD as matrix materials combined with $C_{60}F_{36}$ or F_6-TCNNQ as dopants). Reprinted from Organic Electronics, 15, 365, 2014, Copyright 2014, with permission from Elsevier.
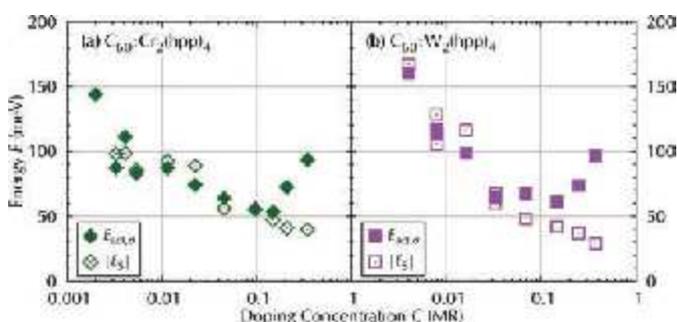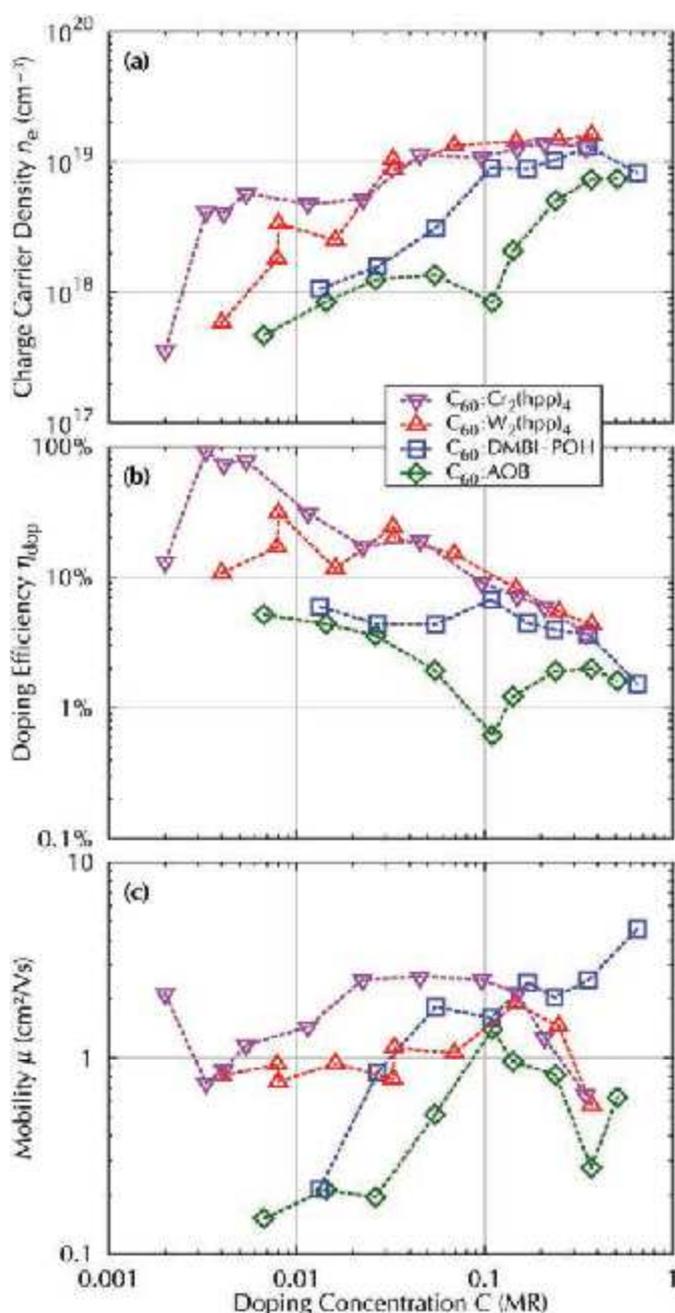

Figure 7: Comparison of Seebeck energies E_S derived from Seebeck measurements and the activation energies E_{act} from temperature dependent conductivity measurements. The two systems compared are C_{60} n-doped with the two metal complexes $Cr_2(hpp)_4$ (a) or $W_2(hpp)_4$ (b). Reprinted from [44] with permission from the author. The data was further published in [30].

Figure 8: Reverse calculation of the charge carrier density n_e, the doping efficiency η_{dop}, and the mobility μ for C_{60} n-doped with different dopants. Reprinted from Physica Status Solidi B, 252, 1877, 2015, Copyright 2015, with permission from John Wiley & Sons Inc.

ing efficiency of 100%.[27] Similarly, using the highest reported mobility value as an upper limit, again lower limits for the charge carrier density and, thus, the doping efficiency can be derived.[37] However, more precise numbers are obtained by taking into account the Seebeck energy.[37] The Fermi level is then reversely calculated in dependence of the doping concentration and the doping efficiency, assuming a Gaussian density of states and Fermi-Dirac statistics. Using the Seebeck energy, which relates the Fermi energy to the transport energy, and the lower limits determined before, the physically allowed range for the transport energy for n-doped C_{60} was narrowed down to approximately 210 meV below the center of the LUMO DOS. Assuming this energy to be constant over the doping concen-

trations used and independent of the dopant compound, the parameters charge carrier density, doping efficiency, and mobility can be calculated reversely (see Figure 8). From these calculations, doping efficiencies of nearly 100% are obtained for the dopant $Cr_2(hpp)_4$ at low concentrations. At very high concentrations of 50 mol%, the doping efficiency decreases to values around 1%. This behavior agrees well with the results from UPS. The higher maximum doping efficiency points to a shallower donor level according to Figure 3c.

E DETERMINATION OF TRAP LEVEL DISTRIBUTIONS

The UPS measurements clearly showed the importance of deep traps for the understanding of doping in organic films. Therefore, the direct measurement of traps is not only important to qualitatively understand the electrical behavior upon doping, but also for the quantitative description of charge transport in undoped films, e.g., for organic solar cell modeling. The direct measurement of traps can furthermore give insights about the material purity, an issue which is often overseen in importance not only for industry, but also for obtaining clear and reproducible results in research.

Therefore, Tietze et al. investigated MeO-TPD of different purity grades, which was achieved by comparing unsublimed material to four times sublimed material which is supposed to possess a reduced amount of impurities compared to the raw material.[38] In UPS measurements, the Fermi level showed a later, but steeper rise with increasing doping concentration (see Figure 9). Modeling this behavior revealed deep trap states at different energies and varying density. Although it is difficult to obtain the exact shape of the trap DOS, it could be concluded that the unpurified material exhibits a fivefold density of deep trap states. However, it is remarkable that even the highly purified material still has a significant density of deep trap states, the origin of which remains unknown.
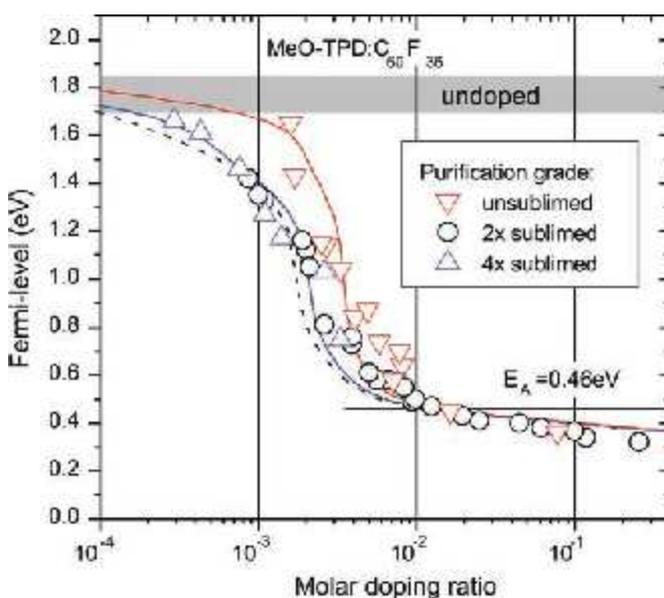
Figure 9: UPS measurement of the Fermi level in differently purified MeO-TPD (unpurified vs. twice and fourfold sublimed) p-doped with $C_{60}F_{36}$. Reprinted from Organic Electronics, 14, 2348, 2013, Copyright 2013, with permission from Elsevier.
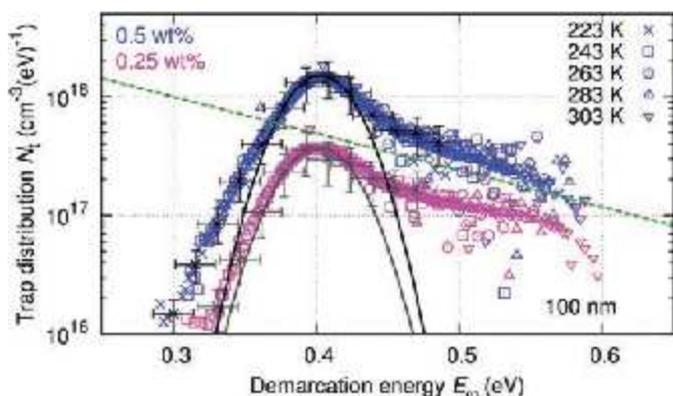
Figure 10: Determination of the (occupied) trap density of states (DOOS) in 100nm thick p-ZnPc:C_{60} blend layers p-doped with $C_{60}F_{36}$ at different doping concentrations and sandwiched between ITO and Al as contacts. The Walter-method[39] was used to derive the distribution from C-f measurements. The green dashed line is taken from a previous publication where the distribution of exponential tail states was determined for the same material system using numerical modeling of j-V characteristics of hole-only devices[40]. Reprinted with permission from Journal of Applied Physics, 117, 245501, 2015. Copyright 2015, AIP Publishing LLC.

Fischer et al. performed trap investigations using impedance spectroscopy.[9] For this technique, it is important to know that only states which are close to the Fermi energy can respond to the electrical stimulus applied. Previously, the required trap filling was achieved either by charge injection or optical charge generation. Here, weak doping was used as an elegant way to selectively populate hole traps and to investigate the resulting density of occupied states (DOOS). For data evaluation, a method developed by Walter et al. was used that is based on temperature dependent capacitance-frequency measurements. [39] For the investigated material system of p-doped ZnPc:C_{60} blend layers, the resulting DOOS showed the main trap distribution at about 0.4eV below the transport energy, followed by an extended exponential tail (see Figure 10), which was also found in previous measurements (green dashed line).[40]

CONCLUSIONS

In this paper, we review our recent advances in the field of molecular doping. The most common picture of doping is extended by a detailed statistical description of the doping process explaining the generally observed low doping efficiencies. It turns out that the consideration of trap states is inevitable for an appropriate theoretical description of the experimental results. By applying a special technique to reduce the molar doping ratio to 10^{-5}, three distinct regions of trap limitation, dopant reserve, and dopant saturation could be observed at different doping concentrations. Besides photoelectron spectroscopy, Seebeck measurements provide further insight into the Fermi level position with respect to the transport level. In combination with conductivity measurements, changes in the doping efficiency can be distinguished from morphological effects. Furthermore, it was possible to locate the transport energy at 210meV below the center of the DOS for n-doped C_{60}. Finally, two methods are shown for the determination of trap levels and trap densities, which is important, e.g., for device modeling and the evaluation of the material purity.

Despite the presented achievements, further understanding is necessary, e.g., on how energy level differences between matrix and dopant affect the doping efficiency. Furthermore, the origin of trap states is still not well understood, which is necessary for future design of high performance material concepts in organic electronics.

REFERENCES

[1] M. Pfeiffer, K. Leo, X. Zhou, J. S. Huang, M. Hofmann, A. Werner und J. Blochwith-Nimoth, „Doped organic semiconductors: Physics and application in light emitting diodes," *Organic Electronics,* Nr. **4**, pp. 89-103, 2003.

[2] K. Walzer, B. Maennig, M. Pfeiffer und K. Leo, „Highly Efficient Organic Devices Based on Electrically Doped Transport Layers," *Chemical Reviews,* Nr. **107**, p. 1233, 2007.

[3] M. Pfeiffer, A. Beyer, T. Fritz und K. Leo, „Controlled doping of phthalocyanine layers by cosublimation with acceptor molecules: A systematic Seebeck and conductivity study," *Applied Physics Letters,* Nr. **73**, pp. 3202-3204, 1998.

[4] J. Blochwith, T. Fritz, M. Pfeiffer, K. Leo, D. M. Alloway, P. A. Lee und N. R. Armstrong, „Interface electronic structure of organic semiconductors with controlled doping levels," *Organic Electronics,* Nr. **2**, pp. 97-104, 2001.

[5] H. Kleemann, R. Gutierrez, F. Lindner, S. Avdoshenko, P. D. Manrique, B. Lüssem, G. Cunibert und K. Leo, „Organic Zener Diodes: Tunneling across the Gap in Organic Semiconductor Materials," *Nano Letters,* Nr. **10**, p. 4929, 2010.

[6] H. Kleemann, S. A. Gutierrez, G. Cunibert, K. Leo und B. Lüssem, „Reverse breakdown behavior in organic pin-diodes comprising C60 and pentacene: Experiment and theory," *Organic Electronics,* Nr. **14**, pp. 193-199, 2013.

[7] B. Lüssem, M. L. Tietze, H. Kleemann, C. Hossbach, J. W. Bartha, A. Zakhidov und K. Leo, „Doped organic transistors operating in the inversion and depletion regime," *Nature communications,* Nr. **4**, p. 2775, 2013.

[8] P. Pahner, H. Kleemann, L. Burtone, M. Tietze, J. Fischer, K. Leo und B. Lüssem, „Pentacene Schottky diodes studied by impedance spectroscopy: Doping properties and trap response," *Physical Review B,* Nr. **88**, p. 195205, 2013.

[9] J. Fischer, D. Ray, H. Kleemann, P. Pahner, M. Schwarze, C. Koerner, K. Vandewal und K. Leo, „Density of states determination in organic donor-acceptor blend layers enabled by molecular doping," *Journal of Applied Physics,* Nr. **117**, p. 245501, 2015.

[10] M. L. Tietze, L. Burtone, M. Riede, B. Lüssem und K. Leo, „Fermi level shift and doping efficiency in p-doped small molecule organic semiconductors: A photoelectron spectroscopy and theoretical study," *Physical Review B,* Nr. **86**, p. 035320, 2012.

[11] I. Salzmann, G. Heimel, S. Duhm, M. Oehzelt, P. Pingel, B. M. George, A. Schnegg, K. Lips, R.-P. Blum, A. Vollmer und N. Koch, „Intermolecular Hybridization Governs Molecular Electrical Doping," *Physical Review Letters,* Nr. **108**, p. 035502, 2012.

[12] I. Salzmann und G. Heimel, „Toward a comprehensive understanding of molecular doping organic semiconductors," *Journal of Electron Spectroscopy and Related Phenomena,* Nr. **204**, pp. 208-222, 2015.

[13] T. Menke, P. Wei, D. Ray, H. Kleemann, B. D. Naab, Z. Bao, K. Leo und M. Riede, „A comparison of two air-stable molecular n-dopants for C60," *Organic Electronics,* Nr. **13**, pp. 3319-3325, 2012.

[14] B. D. Naab, S. Zhang, K. Vandewal, A. Salleo, S. Barlow, S. R. Marder und Z. Bao, „Effective Solution- and Vacuum-Processed n-Doping by Dimers of Benzimidazoline Radicals," *Advanced Materials,* Nr. **26**, pp. 4268-4272, 2014.

[15] S. Guo, S. B. Kim, S. K. Mohapatra, Y. Qi, T. Sajoto, A. Kahn, S. R. Marder und S. Barlow, „n-Doping of Organic Electronic Materials using Air-Stable Organometallics," *Advanced Materials,* Nr. **24**, pp. 699-703, 2012.

[16] S. Zhang, B. D. Naab, E. V. Jucov, S. Parkin, E. G. B. Evans, G. Millhauser, T. V. Timofeeva, C. Risko, J.-L. Brédas, Z. Bao, S. Barlow und S. R. Marder, „n-Dopants Based on Dimers of Benzimidazoline Radicals: Structures and Mechanism of Redox Reactions," *Chemistry: A European Journal,* Nr. **21**, pp. 10878-10885, 2015.

[17] B. Lüssem, M. Riede und K. Leo, „Doping of organic semiconductors," *Physica Status Solidi A,* Nr. **210**, p. 9, 2013.

[18] M. Tietze, *Molecular Doping Processes in Organic Semiconductors investigated by Photoelectron Spectroscopy,* Dissertation, Technische Universität Dresden, 2014.

[19] F. Löser, M. Tietze, B. Lüssem und J. Blochwitz-Nimoth, „Conductivity Doping," in s *OLED Fundamentals: Materials, Devices, and Processing of Organic Light-Emitting Diodes,* 1st Hrsg., D. J. Gaspar und E. Polikarpov, Hrsg., CRC Press, Taylor and Francis, 2015, pp. 189-234.

[20] S.-J. Yoo und J.-J. Kim, „Charge Transport in Electrically Doped Amorphous Organic Semiconductors," *Macromolecular Rapid Communications,* Nr. **36**, pp. 984-1000, 2015.

[21] H. Kleemann, C. Schuenemann, A. A. Zakhidov, M. Riede, B. Lüssem und K. Leo, „Structural phase transition in pentacene caused by molecular doping and its effect on charge carrier mobility," *Organic Electronics,* Nr. **13**, p. 58, 2012.

[22] K. Harada, A. G. Werner, M. Pfeiffer, C. J. Bloom, C. M. Elliott und K. Leo, „Organic Homojunction Diodes with a High Built-in Potential: Interpretation of the Current-Voltage Characteristics by a Generelized Einstein Relation," *Physical Review Letters,* Nr. **94**, p. 036601, 2005.

[23] K. Harada, M. Riede, K. Leo, O. R. Hild und C. M. Elliott, „Pentacene homojunctions: Studies for electron and hole transport properties and related photovoltaic responses," *Physical Review B,* Nr. **77**, p. 195212, 2008.

[24] S. Olthof, W. Tress, R. Meerheim, B. Lüssem und K. Leo, „Photoelectron spectroscopy study of systematically varied doping concentrations in an organic semiconductor layer using a molecular p-dopant," *Journal of Applied Physics,* Nr. **106**, p. 103711, 2009.

[25] T. Glaser, S. Beck, B. Lunkenheimer, D. Donhauser, A. Köhn, M. Kröger und A. Pucci, „Infrared study of the MoO3 doping efficiency in 4,4'-bis(N-carbazolyl)-1,1'-biphenyl (CBP)," *Organic Electronics,* Nr. **14**, pp. 575-583, 2013.

[26] M. L. Tietze, F. Wölzl, T. Menke, A. Fischer, M. Riede, K. Leo und B. Lüssem, „Self-passivation of molecular n-type doping during air exposure using a highly efficient air-instable dopant," *Physica Status Solidi A,* Nr. **210**, pp. 2188-2198, 2013.

[27] T. Menke, D. Ray, H. Kleemann, M. P. Hein, K. Leo und M. Riede, „Highly efficient p-dopants in amorphous hosts," *Organic Electronics,* Nr. **15**, p. 365, 2014.

[28] L. E. Polander, P. Pahner, M. Schwarze, M. Saalfrank, C. Koerner und K. Leo, „Hole-transport material variation in fully vacuum deposited perovskite solar cells," *APL Materials,* Nr. **2**, p. 081503, 2014.

[29] C. Falkenberg, K. Leo und M. Riede, „Improved photocurrent by using n-doped 2,3,8,9,14,15-hexachloro-5,6,11,12,17,18-hexaazatrinaphthylene as optical spacer layer in p-i-n type organic solar cells," *Journal of Applied Physics,* Nr. **110**, p. 124509, 2011.

[30] T. Menke, D. Ray, J. Meiss, K. Leo und M. Riede, „In-situ conductivity and Seebeck measurements of highly efficient n-dopants in fullerene C60," *Applied Physics Letters,* Nr. **100**, p. 093304, 2012.

[31] S. Olthof, S. Mehraeen, S. K. Mohapatra, S. Barlow, V. Coropceanu, J.-L. Brédas, S. R. Marder und A. Kahn, „Ultralow Doping in Organic Semiconductors: Evidence of Trap Filling," *Physical Review Letters,* Nr. **109**, p. 176601, 2012.

[32] S. Schubert, Y. H. Kim, T. Menke, A. Fischer, R. Timmreck, L. Müller-Meskamp und K. Leo, *Solar Energy Materials & Solar Cells,* Nr. **118**, p. 165, 2013.

[33] M. Pfeiffer, T. Fritz, J. Blochwitz, A. Nollau, B. Plönnigs, A. Beyer und K. Leo, *Advances in Solid State Physics,* Nr. **39**, p. 77, 1999.

[34] J. Gao, E. T. Niles und J. K. Grey, „Aggregates Promote Efficient Charge Transfer Doping of Poly(3-hexylthiophene)," *The Journal of Physical Chemistry Letters,* Nr. **4**, pp. 2953-2957, 2013.

[35] M. Tietze, P. Pahner, K. Schmidt, K. Leo und B. Lüssem, „Doped Organic Semiconductors: Trap-Filling, Impurity Saturation, and Reverse Regimes," *Advanced Functional Materials,* Nr. **25**, p. 2701, 2015.

[36] S. M. Sze, Physics of Semiconductor Devices, 2nd edition Hrsg., New York: John Wiley and Sons, 1981.

[37] T. Menke, D. Ray, H. Kleemann, K. Leo und M. Riede, „Determining doping efficiency and mobility from conductivity and Seebeck data of n-doped C60 layers," *Physica Status Solidi B,* Nr. **252**, p. 1877, 2015.

[38] M. L. Tietze, K. Leo und B. Lüssem, „Quantification of deep hole-trap filling by molecular p-doping: Dependence on the host material purity," *Organic Electronics,* Nr. **14**, p. 2348, 2013.

[39] T. Walter, R. Herberholz, C. Müller und H. W. Schock, *Journal of Applied Physics,* Nr. **80**, p. 4411, 1996.

[40] J. Fischer, J. Widmer, H. Kleemann, W. Tress, C. Koerner, M. Riede, K. Vandewal und K. Leo, „A charge carrier transport model for donor-acceptor blend layers," *Journal of Applied Physics,* Nr. **117**, p. 045501, 2015.

[41] A. Opitz, M. Bronner und W. Brütting, „Ambipolar charge carrier transport in mixed organic layers of phthalocyanine and fullerene," *Journal of Applied Physics,* Nr. **101**, p. 063709, 2007.

[42] C. Schünemann, D. Wynands, L. Wilde, M. P. Hein, S. Pfützner, C. Elschner, K.-J. Eichhorn, K. Leo und M. Riede, „Phase separation analysis of bulk heterojunctions in small-molecule organic solar cells using zinc-phthalocyanine and C60," *Physical Review B,* Nr. **85**, p. 245314, 2012.

[43] S. Pfützner, C. Mickel, J. Jankowski, M. Hein, J. Meiss, C. Schuenemann, C. Elschner, A. Levin, B. Rellinghaus, K. Leo und M. Riede, „The influence of substrate heating on morphology and layer growth in C60:ZnPc bulk heterojunction solar cells," *Organic Electronics,* Nr. **12**, p. 435, 2011.

[44] T. Menke, *Molecular Doping of Organic Semiconductors: A Conductivity and Seebeck Study,* Dissertation, Technische Universität Dresden, 2013.